Immunity
Article

Anticancer Chemotherapy-Induced Intratumoral Recruitment and Differentiation of Antigen-Presenting Cells

Yuting Ma,[1,2,3,20] Sandy Adjemian,[1,2,3,20] Stephen R. Mattarollo,[4,5,6,7] Takahiro Yamazaki,[2,3,8] Laetitia Aymeric,[2,3,8] Heng Yang,[1,2,3,9] João Paulo Portela Catani,[1,2,3,10] Dalil Hannani,[2,3,8] Helene Duret,[4,5,6,7] Kim Steegh,[4,5,6,7] Isabelle Martins,[1,2,3] Frederic Schlemmer,[1,2,3] Mickaël Michaud,[1,2,3] Oliver Kepp,[1,2,3] Abdul Qader Sukkurwala,[1,2,3] Laurie Menger,[1,2,3] Erika Vacchelli,[1,2,3] Nathalie Droin,[2,11] Lorenzo Galluzzi,[2,12,13] Roman Krzysiek,[9,14,15] Siamon Gordon,[16] Philip R. Taylor,[17] Peter Van Endert,[18] Eric Solary,[2,3,11] Mark J. Smyth,[4,5,6,7] Laurence Zitvogel,[2,3,8,21,*] and Guido Kroemer[1,12,13,19,21,*]

[1]Institut National de la Santé et de la Recherche Médicale, U848, Villejuif 94805, France
[2]Institut Gustave Roussy, Villejuif 94805, France
[3]Université Paris Sud/Paris 11, Le Kremlin Bicêtre 94270, France
[4]Cancer Immunology Program, Peter MacCallum Cancer Centre, East Melbourne, Victoria 3002, Australia
[5]Diamantina Institute, University of Queensland, Woolloongabba, Queensland 4102, Australia
[6]Immunology in Cancer and Infection Laboratory, Queensland Institute of Medical Research, Herston 4006, Queensland, Australia
[7]School of Medicine, University of Queensland, Herston, Queensland 4006, Australia
[8]Institut National de la Santé et de la Recherche Médicale, U1015, CBT1017, Villejuif 94805, France
[9]Institut National de la Santé et de la Recherche Médicale, UMR 996, LabEx LERMIT, Clamart 92140, France
[10]Laboratorio de Vetores Virais, Instituto do Coração, FM-USP, São Paulo 05403-000, Brasil
[11]Institut National de la Santé et de la Recherche Médicale, U1009, Villejuif 94805, France
[12]Université Paris Descartes/Paris V, Sorbonne Paris Cité, Paris 75006, France
[13]Equipe 11 labellisée par la Ligue Nationale contre le cancer, Centre de Recherche des Cordeliers, Paris 75006, France
[14]Institut Paris-Sud d'Innovation Thérapeutique (IPSIT), Faculté de Pharmacie, Châtenay Malabry 92290, France
[15]Service d'Immunologie biologique, Centre Hospitalier Universitaire de Bicêtre, AP-HP, Le Kremlin Bicêtre 94270, France
[16]Sir William Dunn School of Pathology, University of Oxford, Oxford OX1 3RE, UK
[17]Cardiff Institute of Infection and Immunity, Cardiff University School of Medicine, Cardiff CF14 4YU, UK
[18]Institut National de la Santé et de la Recherche Médicale, U1013, Paris 75015, France
[19]Metabolomics Platform, Institut Gustave Roussy, Villejuif 94805, France
[20]These authors contributed equally to this work
[21]These authors share senior co-authorship
*Correspondence: zitvogel@igr.fr (L.Z.), kroemer@orange.fr (G.K.)
http://dx.doi.org/10.1016/j.immuni.2013.03.003

SUMMARY

The therapeutic efficacy of anthracyclines relies on antitumor immune responses elicited by dying cancer cells. How chemotherapy-induced cell death leads to efficient antigen presentation to T cells, however, remains a conundrum. We found that intratumoral CD11c$^+$CD11b$^+$Ly6C^{hi} cells, which displayed some characteristics of inflammatory dendritic cells and included granulomonocytic precursors, were crucial for anthracycline-induced anticancer immune responses. ATP released by dying cancer cells recruited myeloid cells into tumors and stimulated the local differentiation of CD11c$^+$CD11b$^+$Ly6C^{hi} cells. Such cells efficiently engulfed tumor antigens in situ and presented them to T lymphocytes, thus vaccinating mice, upon adoptive transfer, against a challenge with cancer cells. Manipulations preventing tumor infiltration by CD11c$^+$CD11b$^+$Ly6C^{hi} cells, such as the local overexpression of ectonucleotidases, the blockade of purinergic receptors, or the neutralization of CD11b, abolished the immune system-dependent antitumor activity of anthracyclines. Our results identify a subset of tumor-infiltrating leukocytes as therapy-relevant antigen-presenting cells.

INTRODUCTION

Although it has been generally believed that cytotoxic antineoplastic agents mediate their therapeutic effects in a cancer cell-autonomous fashion, at least some chemotherapeutics inhibit tumor growth also indirectly, via the immune system (Mellman et al., 2011; Schreiber et al., 2011). Thus, a variety of transplantable or chemically induced primary mouse cancers respond more efficiently to anthracyclines when they develop in hosts carrying an intact immune system. In many cases, tumors evolving in immunodeficient mice fail to respond to anthracyclines in conditions in which the same tumors growing in immunocompetent mice do so (Apetoh et al., 2007; Casares et al., 2005; Ghiringhelli et al., 2009; Michaud et al., 2011). Accordingly, clinical studies indicate that anthracycline-killed tumor cells are particularly efficient in stimulating a therapeutic immune response in cancer patients (Zappasodi et al., 2010). Moreover, anthracycline-based neoadjuvant therapy of breast

cancer patients is more effective when the tumor is infiltrated by T cells before the beginning of chemotherapy (Denkert et al., 2010) as well as if chemotherapy causes a significant influx of $CD8^+$ T cells into the tumor bed and/or reduces the accumulation of immunosuppressive regulatory T (Treg) cells (Ladoire et al., 2011).

Several immune effectors that are essential for the therapeutic effect of anthracyclines have been characterized in mouse models. Indeed, the deletion of genes coding for several cytokines (*Il1b, Il17a, Ifng*) or their receptors (*Il1r, Il17r, Ifngr*) abolishes the anticancer effects of anthracyclines, and so does the injection of antibodies that neutralize IL-1β, IL-17, and IFN-γ or that deplete $CD4^+$, $CD8^+$, and γδ T cells (Ghiringhelli et al., 2009; Ma et al., 2011; Michaud et al., 2011; Obeid et al., 2007). Functional experiments suggest a hierarchy of events whereby IL-1β produced by dendritic cells (DCs) allows for the activation of IL-17A-producing γδ T cells, which eventually sustain the accumulation of IFN-γ-producing $CD8^+$ T cells into the tumor bed, 1 week after the chemotherapy has started (Ma et al., 2011).

In contrast to most other cytotoxic chemotherapeutics, anthracyclines stimulate immunogenic cell death. This type of cell death is characterized by a compendium of subtle biochemical changes in the properties of the plasma membrane as well as in the microenvironment of dying cancer cells (Galluzzi et al., 2012; Green et al., 2009). These changes include the preapoptotic exposure of calreticulin (CRT) on the cell surface (which facilitates the engulfment of portions of the dying cells by antigen-presenting cells, APCs) (Gardai et al., 2005) and the postapoptotic release of high mobility group box 1 (HMGB1) from the nucleus (which binds TLR4 receptors and hence stimulates antigen presentation) (Apetoh et al., 2007). We have found that the release of ATP by dying tumor cells is also essential for cell death to be perceived as immunogenic. Indeed, ATP stimulates the recruitment of inflammatory cells into the tumor bed and binds P2RX7 receptors on DCs, thereby facilitating the activation of the NLRP3 inflammasome and the consequent secretion of IL-1β (Ghiringhelli et al., 2009; Martins et al., 2009). Neoplasms in which the pathways leading to CRT exposure or ATP release have been interrupted are refractory to anthracyclines in vivo (Michaud et al., 2011; Panaretakis et al., 2009). Along similar lines, the elimination of TLR4 or P2RX7—as well as that of their intracellular signal transducers MYD88, NLRP3, and caspase-1—from the host immune system is detrimental for the efficacy of anthracycline-based chemotherapy (Ghiringhelli et al., 2009; Obeid et al., 2007).

An abundant literature has described different DC subsets that would be endowed with the capacity to capture dead cell-associated antigens and to stimulate or subvert anticancer immune responses in vivo (Mellman et al., 2011; Palucka and Banchereau, 2012). Beyond plasmacytoid DCs (pDCs), which are mostly tolerogenic (Matta et al., 2010), conventional DCs (cDCs) have been subclassified into inflammatory and BATF3-dependent DCs. The former exhibit a $CD11c^+CD11b^+Ly6C^+$ surface phenotype and play an important role in $CD4^+$ T cell and antimicrobial responses (Kool et al., 2008). The latter express CD8α and/or CD103 and are particularly efficient at engulfing and cross-presenting antigens from dead cells to $CD8^+$ T lymphocytes (Albert et al., 1998; Hildner et al., 2008). The differentiation requirements and functional properties of these DC subsets are highly heterogeneous, suggesting their specific involvement in peculiar sets of immune responses (Mellman et al., 2011; Palucka and Banchereau, 2012).

Here, we addressed the question as to how dead tumor cell antigens are presented to T cells upon anthracycline treatment in vivo. We observed that anthracycline-based chemotherapy stimulates the ATP-driven and purinergic receptor-dependent accumulation of $CD11c^+CD11b^+Ly6C^{hi}$ tumor-infiltrating leukocytes (TILs). This subset of TILs appeared particularly efficient at presenting tumor antigens to $CD8^+$ T cells in vitro and in vivo. Accordingly, experimental manipulations that suppress the recruitment of $CD11c^+CD11b^+Ly6C^{hi}$ cells into the tumor bed, such as the enzymatic degradation of local ATP, the pharmacological inhibition of purinergic receptors, and the injection of CD11b-neutralizing antibodies, all abolished the therapeutic effects of anthracyclines. Our results support the notion that $CD11c^+CD11b^+Ly6C^{hi}$ TILs are essential for the efficacy of anthracycline-based chemotherapy.

RESULTS

Chemotherapy-Induced Recruitment of Myeloid Cells into the Tumor Bed

When murine MCA205 fibrosarcomas growing in syngenic C57Bl/6 mice reached a diameter of 5–10 mm, they contained <1% cells with the surface phenotype of mature DCs ($CD11c^+CD86^+$), macrophages ($F4/80^+CD169^+$), and granulocytes ($CD11b^+Ly6G^+$) and <10% of cells bearing the general myeloid marker CD11b, as detectable by in situ immunofluorescence and confocal microscopy. Systemic chemotherapy with the prototypic anthracycline mitoxantrone (MTX) led to a rapid (12 hr) increase in the prevalence of $CD11c^+CD86^+$ cells, followed by a slightly delayed (48 hr) accumulation of $F4/80^+CD169^+$ and $CD11b^+Ly6G^+$ TILs (Figures 1A and 1B). These three cell types were localized in the immediate proximity of dying tumor cells, as shown by the distance to the closest cancer cell positive for cleaved caspase-3 (a marker of apoptosis), which was significantly shorter than that to the closest living cancer cell (Figures 1C and 1D). As previously reported (Chow et al., 2011), $CD11c^+CD86^+$ cells were significantly more elongated than $F4/80^+CD169^+$ and $CD11b^+Ly6G^+$ TILs, whereas both $CD11c^+CD86^+$ and $F4/80^+CD169^+$ cells were larger than $CD11b^+Ly6G^+$ cells (Figure 1C). Mechanic and enzymatic dissociation of tumors followed by immunofluorescence and cytofluorometric analyses confirmed the recruitment of myeloid ($CD45^+CD11b^+$) cells, and more specifically DCs ($CD11c^+MHC\text{-}II^+$), bearing monocytic markers ($Ly6C^+7/4^+$), but not of other cell types such as Treg cells ($CD3^+CD4^+FOXP3^+$) or Th17 cells ($CD3^+CD4^+IL\text{-}17^+$), into the tumor bed 2 days after chemotherapy with doxorubicin (DX, another widely employed anthracycline), correlating with the induction of cancer cell death (Figures 1E and 1F; Figure S1 available online; data not shown). Altogether, these results indicate that distinct classes of myeloid cells accumulate in the tumor bed after chemotherapy.

Critical Involvement of ATP and Purinergic Receptors in the Recruitment of Myeloid Cells

To elucidate the mechanisms accounting for the chemotherapy-induced recruitment of myeloid cells into the tumor bed, we

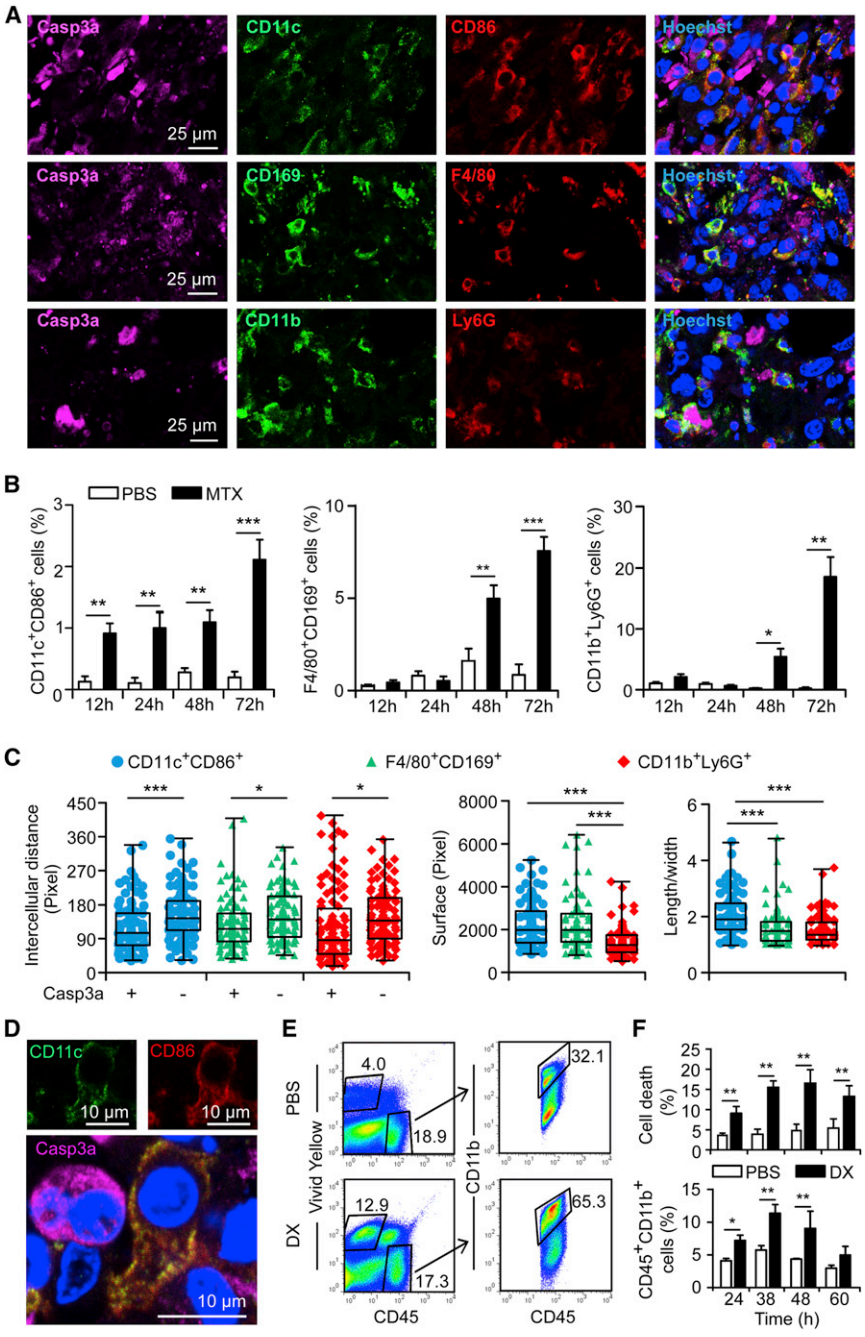

Figure 1. Chemotherapy Induces the Accumulation of Myeloid Cells in Close Proximity to Dying Cells

Wild-type C57BL/6 mice bearing MCA205 fibrosarcomas were treated with mitoxantrone (MTX) i.p. (A–D), doxorubicin (DX) i.t. (E, F), or with an equivalent volume of PBS, as a single injection. At the indicated time points (48 hr where not indicated), tumors were harvested and processed for the detection of the indicated proteins by immunofluorescence microscopy (A–D) or for cytofluorometric determinations (E, F). Hoechst 33342 was employed as nuclear counterstaining.

(A) Representative images (scale bars represent 25 μm).

(B) Quantitative data on the frequency of the indicated cell populations (means ± SEM, in 10 viewfields for at least n = 10 distinct tumors).

(C) The indicated myeloid cell populations were quantitatively characterized for their intercellular distance from tumor cells displaying (+) or not (–) activated caspase 3 (Casp3a) (left), cell surface (middle), and the length/width ratio (right), as determined by morphometric methods. Boxplots report the lower and upper quartile plus the median value. Whiskers indicate min and max values.

(D) A $CD11c^+CD86^+$ dendritic cell (DC) in the close proximity of a dying tumor cell (scale bars represent 10 μm).

(E) Representative dot plots of cells from PBS-treated and DX-treated tumors are depicted, including dead cells that incorporate the exclusion dye vivid yellow and living $CD11b^+CD45^+$ tumor-infiltrating leucocytes. Numbers indicate the percentage of cells found within the corresponding gate.

(F) The corresponding quantitative data (means ± SEM).

*p < 0.05, **p < 0.01, ***p < 0.001 (unpaired, two-tailed Student's t test). See also Figure S1.

took advantage of MCA205 cells that had been engineered to express the ecto-ATPase CD39 on the cell surface (Michaud et al., 2011; Stagg and Smyth, 2010). In response to MTX-based chemotherapy, $CD39^+$ MCA205 tumors failed to attract $CD11c^+CD86^+$, $F4/80^+CD169^+$, or $CD11b^+Ly6G^+$ cells, whereas control tumors (derived from MCA205 cells transduced with an empty vector) did so (Figure 2A), indicating that ATP is essential for the recruitment of these myeloid cells in the tumor bed. Tumors developing in mice that lack the metabotropic purinergic receptor P2Y2 (which mediates the chemotaxis of monocytes toward apoptotic cells) (Chekeni et al., 2010; Elliott et al., 2009) also failed to accumulate $CD11c^+CD86^+$, $F4/80^+CD169^+$, and $CD11b^+Ly6G^+$ cells after the administration of MTX (Figure 2B). Suramin, a nontoxic broad-spectrum inhibitor of purinergic receptors (Elliott et al., 2009), prevented the recruitment of both $CD11c^+CD86^+$ and $CD11b^+Ly6G^+$ cells yet failed to affect the frequency, polarization, and function of $F4/80^+CD169^+$ macrophages (Figures 2C and S2). The local overexpression of CD39 (Figure 2D) and the administration of suramin (Figure 2E) abolished the growth-inhibitory effects of systemic MTX-based chemotherapy in a similar fashion, underscoring the functional importance of ATP and purinergic receptors for the therapeutic efficacy of anthracyclines.

Identification of APCs among Tumor-Infiltrating Myeloid Cells

The ablation of tumor-draining lymph nodes shortly after chemotherapy or even before tumor implantation failed to reduce the efficacy of anthracycline-based chemotherapy (Figure S3A). Similar results were obtained upon the injection of a lymphotoxin

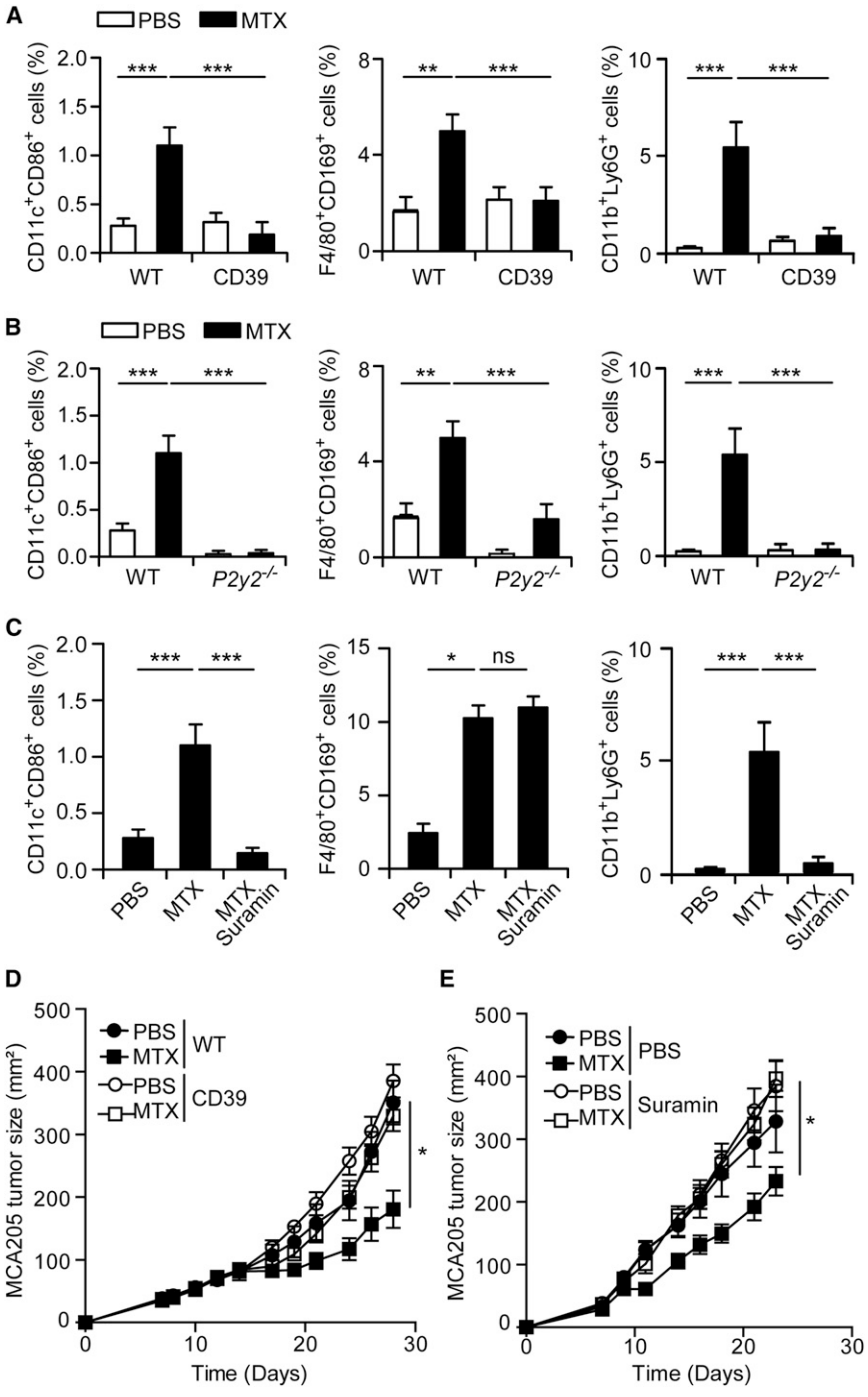

Figure 2. Obligate Contribution of ATP and Purinergic Receptors to Anthracycline-Induced Accumulation of Myeloid Cells and Chemotherapeutic Outcome

(A–C) Wild-type (WT) (A–C) or *P2y2*$^{-/-}$ (B) C57BL/6 mice bearing WT (A–C) or CD39-expressing (CD39) (B) MCA205 fibrosarcomas received mitoxantrone (MTX) i.p. or an equivalent volume of PBS, either alone (A–C) or combined with suramine i.v. (C), and tumor-infiltrating leucocytes of the indicated phenotypes were quantified 48 hr later by immunofluorescence microscopy. Quantitative data are represented as means ± SEM; *$p < 0.05$, **$p < 0.01$, ***$p < 0.001$; ns, nonsignificant (unpaired, two-tailed Student's t test).

(D and E) WT C57BL/6 mice were inoculated s.c. with WT (D, E) or CD39 (D) MCA205 cells and tumor size was routinely assessed. When tumor became palpable (surface area = 25 mm^2), mice received MTX i.p. or an equivalent volume of PBS, either alone (D, E) or combined with suramine i.v. (E). Quantitative data are represented as means ± SEM; *$p < 0.05$ (Mann-Whitney U test).

See also Figure S2.

β receptor-Fc fusion protein (LTβR-Fc), serving as a decoy for LTβ (Figure S3B), as well as after the simultaneous neutralization of IL-7 and IL-7R (Figure S3C), two measures that abolish the formation of tertiary lymphoid structures (Gräbner et al., 2009; Meier et al., 2007). Moreover, anthracycline-based chemotherapy failed to enhance (and actually it reduced) the number of TILs exhibiting the surface phenotype of lymphoid tissue inducers (CD45$^+$B220$^-$CD11c$^-$CD3$^-$CD4$^+$CD127$^+$) (Figure S3D), yet led to the activation of tumor-infiltrating CD8$^+$ T cells and adoptively transferred ovalbumin (OVA)-specific OT-I cells against OVA-expressing MCA205 tumors from within the tumor bed (Figure S3E). In this model, the proliferation of intratumoral OT-I cells induced by chemotherapy was not reduced by the surgical removal of draining lymph nodes. Moreover, chemotherapy did not increase the frequency of CD11c$^+$MHC-II$^+$ cells detectable in tumor-draining lymph nodes (data not shown). Altogether, these results suggest that the presentation of tumor antigens relevant to the success of anticancer chemotherapies may take place in the tumor bed itself, even in the absence of draining lymph nodes and tertiary lymphoid structures.

To determine the origin of intratumoral DCs (CD11c$^+$MHC-II$^+$ cells), we established MCA205 cancers in CD45.1 mice, treated them by vehicle or chemotherapy, transplanted them 1 day later to isogenic CD45.2 C57BL/6 recipients, and measured the frequency of tumor-sessile (CD45.1$^+$) versus freshly recruited (CD45.2$^+$) DCs. The ratio of recipient-derived (CD45.2$^+$) versus donor-derived (CD45.1$^+$) CD11c$^+$MHC-II$^+$ DCs was increased by chemotherapy, supporting the notion that chemotherapy triggers the recruitment of DC precursors rather than a mere in situ differentiation of pre-existing myeloid cells (data not shown). To characterize the intratumoral APCs responsible for the chemotherapy-relevant presentation of tumor antigens, we engineered mouse CT26 colon cancers cells to express EGFP on the inner leaflet of the plasma membrane owing to the addition of a myristoylation motif (Figure 3A). Upon the administration of DX, a significant fraction of CD45$^+$

TILs, especially among the $CD11b^+Ly6C^{hi}Ly6G^-$ subset, became positive for EGFP (Figure 3B). In this context, $CD11b^+Ly6C^{hi}Ly6G^-$ cells exhibited a stronger EGFP positivity and higher expression of CD11c than did $CD11b^+Ly6C^{lo}Ly6G^-$ cells and $CD11b^+Ly6G^+$ granulocytes. Moreover, $CD11b^+Ly6C^{hi}Ly6G^-$ cells clearly manifested the presence of EGFP in the cytoplasm, an indication of the uptake of antigens from tumor cells. Of note, the frequency of $CD11b^+Ly6C^{lo}Ly6G^-$ cells, which also engulfed tumor antigens, did not increase in response to chemotherapy (Figures 3C and 3D).

$CD11b^+Ly6C^{hi}Ly6G^-$ cells accumulated in the tumor bed after chemotherapy in an ATP-dependent fashion (data not shown), mostly exhibited DC markers ($CD11c^+MHC\text{-}II^{int}F4/80^{lo}$), and stained positive for 7/4, CD103, CD172a, CCR2, and CX3CR1, but lacked CD205 expression (Figure S4). When we treated palpable OVA-expressing MCA205 fibrosarcomas with anthracyclines, the frequency of $Ly6C^{hi}Ly6G^-$ cells (as determined upon the cytofluorometric purification of the $Ly6C^{hi}Ly6G^-$, $Ly6C^{lo}Ly6G^-$, and $Ly6G^+$ subsets of $CD11b^+$ TILs) increased, and these cells turned out to be particularly efficient in stimulating the production of IFN-γ by MHC class I-restricted OVA-specific OT-I cells in vitro. Moreover, $Ly6C^{hi}Ly6G^-$ cells recovered from DX-treated OVA-expressing tumors were much more efficient than their $Ly6C^{lo}Ly6G^-$ counterparts as well as than $Ly6G^+$ cells in stimulating the secretion of IL-2 by MHC class I-restricted OVA-specific B3Z hybridomas (Figure 3E). This effect was antigen specific (as shown by the fact that $Ly6C^{hi}Ly6G^-$ cells recovered from OVA-negative tumors failed to stimulate B3Z cells) and required MHC molecules. $Ly6C^{hi}Ly6G^-$ TILs recovered from homozygous $H2K^bD^b$-deficient hosts (Pérarnau et al., 1999) failed indeed to elicit IL-2 production by B3Z cells. Noteworthy, tumor or stromal cells (namely, the $CD45^-$ cell subset harvested from anthracycline-treated OVA-expressing MCA205 tumors) failed to directly activate OT-I or B3Z ex vivo (Figure 3E).

Next, we purified $Ly6C^{hi}Ly6G^-$, $Ly6C^{lo}Ly6G^-$, and $Ly6G^+$ TILs (all sharing the surface phenotype $CD45^+B220^-CD3^-CD11b^+$) from vehicle-treated or DX-treated OVA-expressing MCA205 tumors and adoptively transferred them into naive mice that were challenged 10 days later with living OVA-expressing MCA205 cells. Importantly, only $Ly6C^{hi}Ly6G^-$ (but neither $Ly6C^{lo}Ly6G^-$ nor $Ly6G^+$) TILs harvested from anthracycline-treated tumors were capable of reducing the incidence and growth of tumors (Figure 3F), indicating that this population indeed contains functionally competent APCs. Accordingly, purified $Ly6C^{hi}Ly6G^-$ TILs exhibited a significant increase in the expression of genes relevant to MHC class I- or II-restricted antigen presentation after DX-based chemotherapy, in vivo (data not shown). Altogether, these results identify $CD11b^+Ly6C^{hi}Ly6G^-$ TILs as the cells that accumulate in the tumor bed to exert APC functions in response to anthracycline treatment.

ATP-Dependent Differentiation of Myeloid Precursors into Dendritic Cells

Chemotherapy with anthracyclines induced the accumulation of $CD34^+c\text{-}Kit^+Sca\text{-}1^+CD11b^{int}CD16/32^{+/-}$ multipotent progenitors (MPPs) and $CD34^+c\text{-}Kit^+Sca\text{-}1^-CD11b^{int}CD16/32^{hi/lo}$ myeloid precursors (MPs) in tumors (data not shown). A more detailed characterization of myeloid TILs ($CD45^+B220^-CD3^-CD11b^+$) revealed that several cell subsets, including $Ly6C^{hi}Ly6G^-$, $Ly6C^{lo}Ly6G^-$, and $Ly6G^+$ cells, contained a significant fraction of cells exhibiting a common myeloid progenitor (CMP) or granulocyte-monocyte progenitor (GMP) phenotype ($CD34^+c\text{-}Kit^+Sca\text{-}1^-CD16/32^+$), and more so after chemotherapy. Of note, the frequency of such CMP or GMP-like cells among $Ly6C^{hi}Ly6G^-$ TILs was reduced by the presence of the ecto-ATPase CD39 on the surface of tumor cells (Figure 4A). Quantitative RT-PCR analyses confirmed that transcription factors and regulators associated with the monocytic lineage (i.e., PU.1, Nab2) (Auffray et al., 2009; Laslo et al., 2006) were upregulated, in particular among $Ly6C^{hi}Ly6G^-$ TILs, after DX-based chemotherapy, and that this increase was abolished by the expression of CD39 (Figure 4B). The expression of transcription factors relevant for the differentiation of granulocytes (i.e., Gfi1) (de la Luz Sierra et al., 2010; Laslo et al., 2006) or the megakaryocytic-erythrocytic lineage (i.e., Gfi1b and Gata1) (Yu et al., 2009) was increased in response to DX, yet predominantly among $Ly6G^+$ cells and independently of CD39 (Figure 4B). In line with these observations, $Ly6C^{hi}Ly6G^-$ (but not $Ly6G^+$) TILs recovered from tumors and propagated in dedicated methylcellulose cloning conditions could form colonies that were highly proliferative (Figures 4C–4E). These proliferating cells retained GMP markers and acquired the morphology and phenotype of monocytes (Figure 4F and data not shown). Anthracycline-based chemotherapy dramatically increased the frequency of colony-forming units among $Ly6C^{hi}Ly6G^-$ TILs, an effect that was precluded by the expression of CD39 by tumor cells (Figure 4C). Thus, chemotherapy appears to induce the recruitment of GMPs with monocytic differentiation potential at the tumor site, in an ATP-dependent manner.

Chemotherapy Induced the ATP-Dependent Differentiation of $CD11b^+Ly6C^{hi}$ Tumor-Infiltrating Leucocytes into Inflammatory DC-like Cells

We characterized the impact of the intratumoral milieu on the differentiation of $Ly6C^{hi}Ly6G^-$ TILs into bona fide DCs, placing special emphasis on ATP. $Ly6C^{hi}Ly6G^-$ TILs were recovered from tumors established in CD45.2 C57BL/6 mice and treated with anthracyclines and then adoptively transferred into MCA205 tumors growing in congenic CD45.1 mice that were treated with either vehicle (PBS) or DX. Upon transfer into tumors that did not receive chemotherapy, the initial $CD45.2^+Ly6C^{hi}Ly6G^-$ cell population mostly differentiated into $CD45.2^+Ly6G^+$ granulocytes. In contrast, upon transfer into anthracycline-treated tumors, a fraction of $Ly6C^{hi}Ly6G^-$ TILs maintained the $Ly6C^{hi}Ly6G^-$ phenotype and acquired surface markers of DCs (namely CD11c and MHC class II molecules) (Figures 5A–5C). Similar results were obtained in a syngeneic (CD45.2) system in which $Ly6C^{hi}Ly6G^-$ or $Ly6G^+$ TILs recovered from anthracycline-treated tumors were labeled with CFSE and then transferred into anthracycline-treated MCA205 tumors. A substantial fraction of such $Ly6C^{hi}Ly6G^-CFSE^+$ cells acquired the expression of CD11c and CD86 (Figures 5D and 5E). Failure to provide chemotherapy as well as transfer into CD39-expressing tumors reduced the frequency of the adoptively transferred cells that could be recovered from the tumor bed (Figures 5E and 5F). As a control, the $Ly6G^+$ population, which did not contain significant

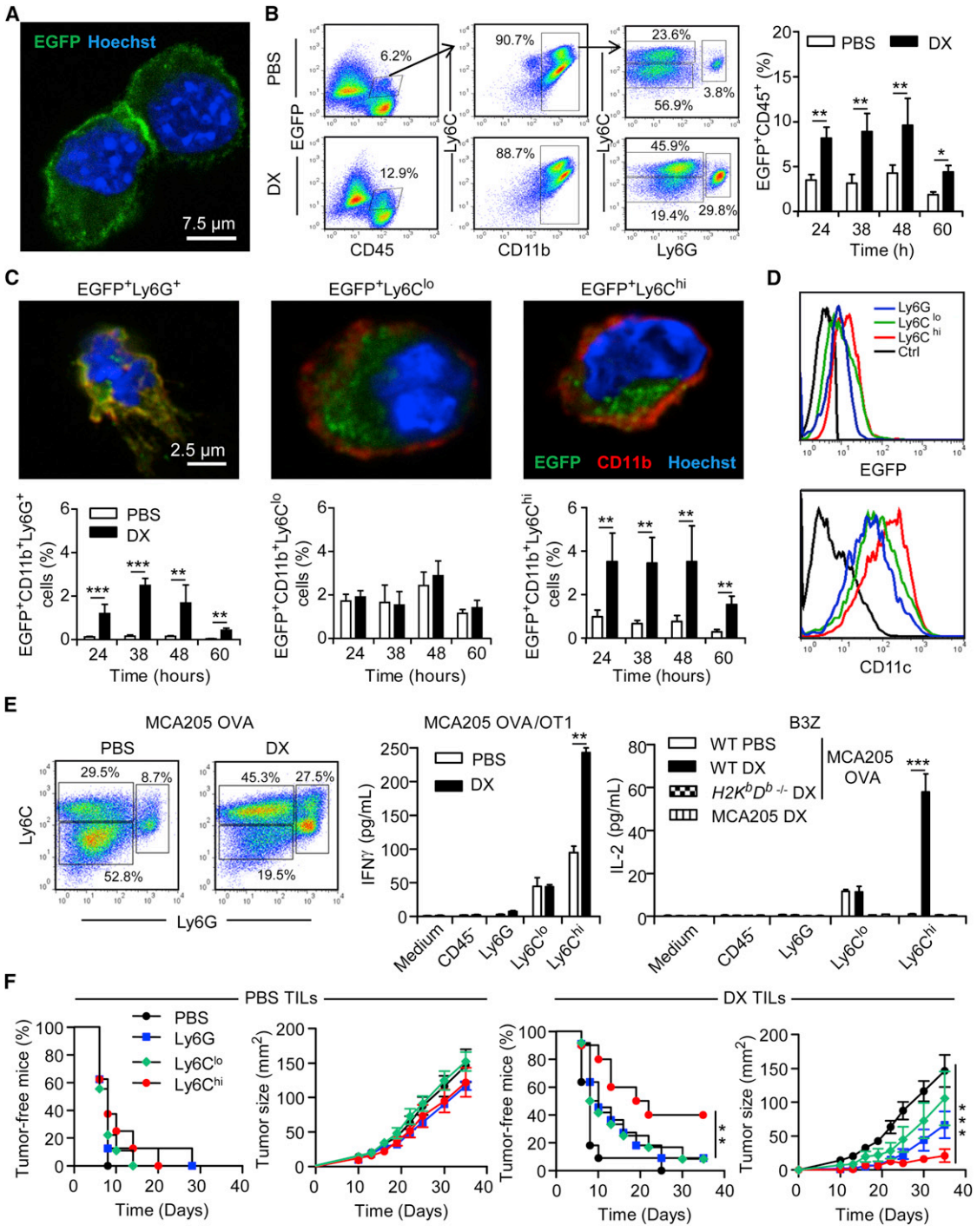

Figure 3. Chemotherapy Promotes the Uptake and Presentation of Tumor Antigens by CD11c$^+$Ly6C^{hi}Ly6G$^-$ Tumor-Infiltrating Leucocytes

(A–D) BALB/c mice bearing MyrPalm-EGFP-expressing CT26 tumors were treated with doxorubicin (DX) i.t. or with an equivalent volume of PBS. At the indicated time points (38 hr, where not indicated), tumors were harvested and processed for immunofluorescence studies (A and C) or cytofluorometric determinations (B and D).

(A) MyrPalm-mEGFP-expressing mouse colon carcinoma CT26 cells, exhibiting a plasma membrane-restricted distribution of EGFP (scale bar represents 7.5 μm).

(B) Representative dot plots of EGFP$^+$CD45$^+$ tumor-infiltrating leucocytes (TILs) stained for CD11b, Ly6C, and Ly6G are illustrated on the left, and quantitative data are reported on the right.

(C) Uptake of tumor antigens (as exemplified by EGFP) by myeloid cells of the indicated phenotype (top, scale bar represents 2.5 μm) and quantitative kinetic data (bottom).

(D) Representative cytofluorometric distribution of EGFP and CD11c mean fluorescence intensity for the indicated myeloid cell populations.

(A and C) Hoechst 33342 was employed as nuclear counterstaining.

(legend continued on next page)

numbers of precursor cells (Figure 4C), failed to generate $CD11c^+CD86^+$ cells upon adoptive transfer into anthracycline-treated tumors (Figure 5E). Altogether, these results suggest that chemotherapy-elicited ATP release within the tumor bed can skew the differentiation of $CD11b^+Ly6C^{hi}Ly6G^-$ TILs toward a $CD11c^+$ DC-like phenotype, hence subverting their default pathway leading to the generation of $Ly6G^+$ granulocytes, which we observed within PBS-treated tumors (Figure 5C).

To get further insights into this issue, we cocultured control or $CD39^+$ MCA205 cells that were optionally treated with anthracyclines in vitro (CD39 expression abolished the anthracycline-driven accumulation of extracellular ATP; Figure 5G) with bone marrow-derived $CD11b^+Ly6C^{hi}Ly6G^-$ cells, a substantial part (around 30%–40%) of which showed a GMP phenotype. Only anthracycline-treated $CD39^-$ (but not $CD39^+$) tumor cells stimulated such a subset to express the monocyte-relevant transcription factor PU.1 (Figure S5). Along similar lines, only $CD39^-$ cells treated with anthracyclines (but neither anthracycline-treated $CD39^+$ cells nor untreated $CD39^-$ cells) enhanced the differentiation of $CD11b^+Ly6C^{hi}Ly6G^-$ bone marrow cells into $CD11b^+Ly6C^+$ monocytes (de facto limiting granulocytic differentiation) and allowed for the generation of a significant number of $CD11c^+$MHC-II^+ DC-like cells (Figures 5H and 5I). This skew in differentiation from $Ly6G^+$ granulocytes to cells with a $CD11b^+CD11c^+$ DC phenotype was reduced by the pannexin 1 inhibitor DIDS (which limits ATP release from dying cells) and by several purinergic receptor antagonists including oxidized ATP and suramin, but neither by recombinant IL-1 receptor antagonist (IL-1RA) nor by the TNF-α antagonist etanercept (Figures 5J and 5K). These results underscore the importance of extracellular ATP and purinergic receptors for the generation of DCs in response to anthracyclin-based chemotherapy.

Identification of the DC Subset Underlying Chemotherapy-Induced Anticancer Immune Responses

Multiple distinct DC subsets might contribute to the presentation of dead cell antigens to T cells. To identify the specific DC population that is relevant to anticancer chemotherapy, we first injected a PDCA-1-specific antibody into tumor-bearing mice that had received anthracyclin-based chemotherapy. Although the PDCA-1-targeting antibody effectively depleted plasmacytoid DCs (data not shown), this treatment neither suppressed the chemotherapy-induced accumulation of $CD11b^+CD11c^-GFP^+$ TILs (in mice that express GFP under the control of the CD11c promoter) (Figure 6A) nor reduced the efficacy of anthracycline- and oxaliplatin-based chemotherapy (Figures 6B and 6C). Along similar lines, the deletion of the transcription factor Batf3, which is essential for the generation of $CD8\alpha^+CD103^+$ Langerin$^+$ DCs (Hildner et al., 2008), failed to reduce MTX-induced tumor infiltration by $CD11b^+CD11c^+$ TILs (Figure 6D), and tumors implanted in wild-type and *Batf3*$^{-/-}$ mice responded to chemotherapy in an indistinguishable fashion (Figure 6E). In contrast, the injection of a CD11b-blocking antibody strongly reduced the frequency of $CD11b^+Ly6C^{hi}$ cells in the peripheral blood (Figure 6F), as well as of $CD11b^+CD11c^-GFP^+$ cells infiltrating MTX-treated tumors (Figure 6G). In accord with the finding that $CD11b^+CD11c^+$ TILs are responsible for chemotherapy-related antigen presentation and antitumor protection in vivo (Figure 3), neutralization of CD11b abolished the anticancer effect of anthracyclines in four different tumor models, namely MCA205 fibrosarcomas and AT3 mammary cancers, both of which grow in C57BL/6 mice (Figures 6H and 6I), F244 sarcoma cells, which form tumors in 129/Sv mice (Figure 6J), and H2N100 mammary cancers, developing in BALB/c mice (Figure 6K). In contrast, the depletion of macrophages (with clodronate-containing liposomes) or neutrophils (with the 1A8 antibody) had no or only minor effects, respectively, on the efficacy of chemotherapy (Figure S6 and data not shown). Altogether, these results underscore the fundamental importance of inflammatory DC-like $CD11b^+CD11c^+$ cells for the efficacy of anticancer chemotherapy.

DISCUSSION

Our findings provide at least three lines of evidence indicating that a peculiar subtype of TILs, namely $CD11c^+CD11b^+Ly6C^{hi}$ cells, which share some of the characteristics of inflammatory DCs (Cheong et al., 2010), is particularly important for the induction of anticancer immune responses by anthracyclines. First, $CD11c^+CD11b^+Ly6C^{hi}$ cells were recruited into the tumor bed as early as 12 hr after chemotherapy. Second, manipulations aimed at preventing the intratumoral accumulation of such cells, including (1) the local overexpression of the ATP-degrading enzyme CD39, (2) the pharmacological blockade of purinergic receptors, and (3) the neutralization of CD11b with a specific antibody, abolished the immune-dependent anticancer effects of anthracyclines. Third, functional experiments revealed that $CD11c^+CD11b^+Ly6C^{hi}$ TILs are particularly efficient in capturing and presenting tumor cell antigens and that such cells—once adoptively transferred into naive mice—can confer protection against a challenge with living tumor cells.

ATP appears to be particularly important for the infiltration of myeloid TILs into the tumor bed upon anthracycline-based chemotherapy. Indeed, palpable tumors generated from cancer cells manipulated to overexpress the ecto-ATPase CD39 failed to recruit TILs of various types, including cells with a DC-like, macrophage-like, or granulocyte surface phenotype in response to anthracyclines. In line with recent results (Chen et al., 2006), P2Y2 turned out to be essential for the chemotherapy-induced

(B and C) Quantitative data are represented as means ± SEM; *$p < 0.05$, **$p < 0.01$, ***$p < 0.001$ (unpaired, two-tailed Student's t test).
(E) WT or *H2K*^{b}*D*$^{b-/-}$ C57BL/6 mice bearing OVA-expressing (OVA) MCA205 fibrosarcomas were treated as in (A)–(D) and $CD11b^+$ TILs were purified by cytofluorometry 38 hr after chemotherapy upon staining with Ly6C- and Ly6G-specific antibodies (gating exemplified on the left). Sorted cells were cocultured with OT-I cells for 72 hr or with OVA-specific T cell hybridoma B3Z cells for 36 hr and supernatants were assessed for interferon-γ (IFN-γ, middle) and interleukin-2 (IL-2, right) levels. Numbers indicate the percentage of cells found within the corresponding gate. Quantitative data are represented as means ± SEM; **$p < 0.01$, ***$p < 0.001$ (unpaired, two-tailed Student's t test).
(F) Alternatively, PBS (negative control) or myeloid cells sorted as in (E) from PBS-treated (left) or DX-treated (right) tumors were inoculated in the footpad of naive WT C75BL/6 mice, which were rechallenged 10 days later with living OVA MCA205 tumor cells. Tumor incidence and growth were then routinely assessed. Results from one representative experiment out of three independent ones involving ten mice/group is depicted. **$p < 0.01$, ***$p < 0.001$ (log-rank test).
See also Figure S3.

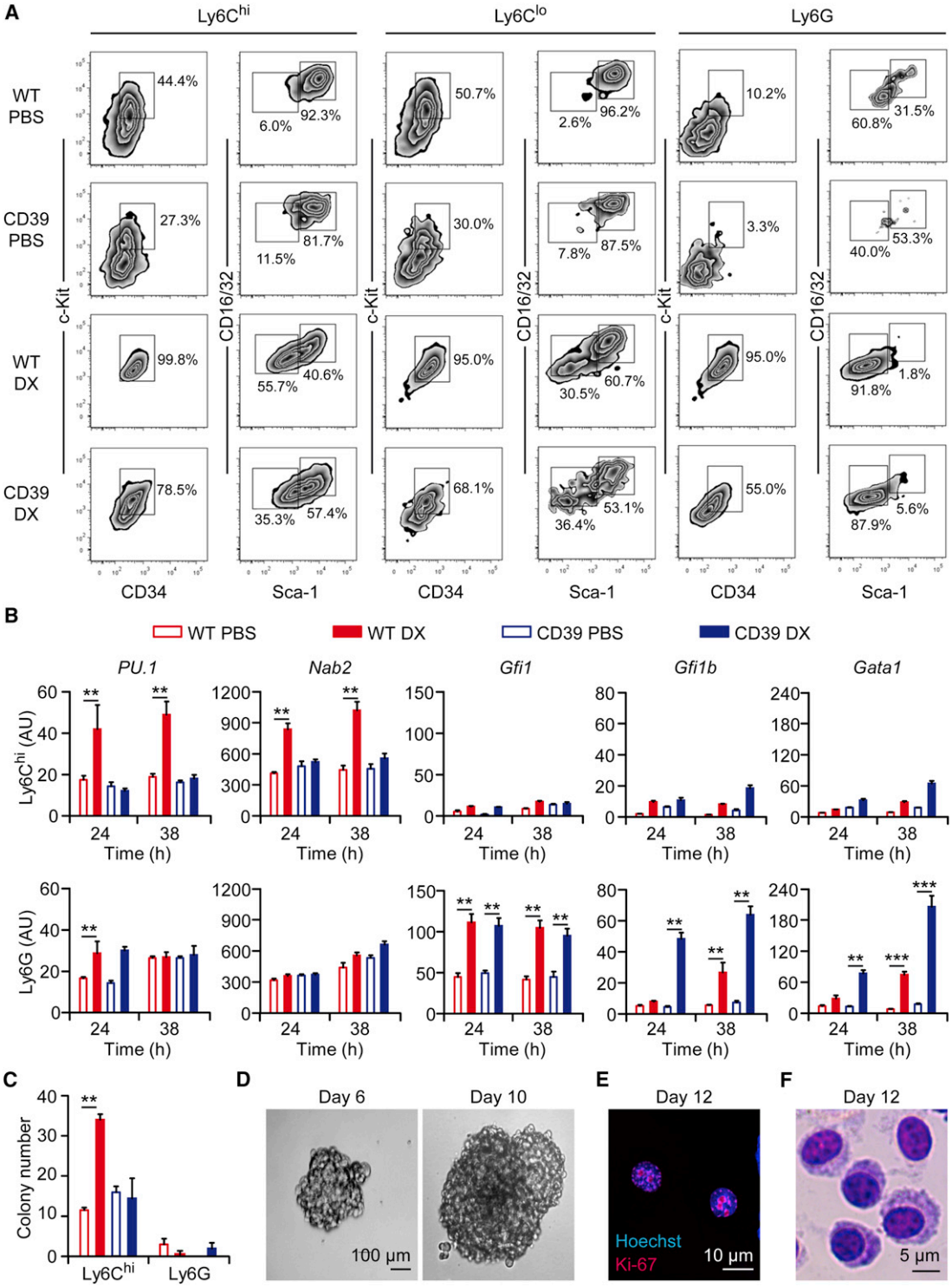

Figure 4. Chemotherapy-Induced and ATP-Dependent Enrichment of Granulocyte Monocyte Progenitors in Tumor-Infiltrating Leucocytes

C57BL/6 mice bearing wild-type (WT) or CD39-expressing (CD39) MCA205 fibrosarcomas were treated with doxorubicin (DX) i.t. or with an equivalent volume of PBS. (A) 24 hr later, tumors were harvested and the expression of hematopoietic progenitor markers (CD34, c-Kit, Sca-1, and CD16/32) on $CD45^+CD3^-B220^-CD11b^+$ ($Ly6C^{hi}$, $Ly6C^{lo}$, or $Ly6G^+$) tumor-infiltrating cells was analyzed by flow cytometry. Numbers indicate the percentage of cells found within the corresponding gate. Please note that the $CD34^+c\text{-}Kit^+Sca\text{-}1^-CD16/32^+$ phenotype marks common myeloid progenitors (CMPs) as well as granulocyte-monocyte progenitor (GMPs). (B–F) Alternatively, tumors were harvested at the indicated time points (24 hr, where not indicated), and $CD11b^+Ly6C^{hi}$ and $CD11b^+Ly6G^+$ tumor-infiltrating cells were characterized by RT-PCR for the expression of transcriptional regulators (the monocytic factors PU.1 and Nab-2, the granulopoietic factor Gfi-1, and the erythroid and megakaryocytic factors Gata-1 and Gfi1b) (B) or used in clonogenic assays in methylcellulose-based medium (C–F).

(legend continued on next page)

recruitment of TILs to the tumor bed. In contrast, pharmacological inhibition of purinergic receptors with suramin was more efficient in blocking the chemotherapy-elicited infiltration of tumors by DCs and granulocytes than that by macrophages.

Lymphadenectomy failed to affect the therapeutic response of mice to anthracyclines, nor did the neutralization or blockade of the LTβ-LTβR and IL-7-IL-7R systems. These findings suggest that TILs accumulating in the tumor upon chemotherapy can mediate anticancer immune responses without the need to migrate into lymph nodes nor to form tertiary lymphoid structures. It appears therefore plausible that $CD11c^+CD11b^+Ly6C^{hi}$ TILs may efficiently process and present tumor cell antigens (which they readily take up in vivo, as indicated by the transfer of cancer cell-derived EGFP into their cytoplasm) locally, within the tumor bed.

ATP can be released from dying cells in response to physiological cell death inducers (such as glucocorticoids acting on thymocytes) (Chekeni et al., 2010; Elliott et al., 2009) or therapeutic interventions including radiotherapy and chemotherapy (Martins et al., 2009). Within tissues, the concentration of extracellular ATP ($[ATP]_e$) in the proximity of stressed and dying cells is believed to decrease along a steep gradient, owing to the presence of ecto-ATPases that are expressed by a variety of cell types (including $FOXP3^+$ Treg and Th17 cells) (Borsellino et al., 2007; Chalmin et al., 2012; Schreiber et al., 2011) as well as of soluble, plasmatic ATPases (Yegutkin et al., 2003). Such a pattern of $[ATP]_e$ may facilitate the migration of myeloid cells toward dying cells. Our results are compatible with the notion that ATP acts as a specific chemotactic (and perhaps chemotropic) signal that emanates from dying cells. Indeed, $CD11c^+CD11b^+Ly6C^{hi}$ TILs, as well as other myeloid populations, were found within nests of dying cells, and—more precisely—in close proximity of cells that manifested apoptotic caspase-3 activation (Kroemer et al., 2007). Moreover, ATP may affect the differentiation of pluripotent myeloid cell populations recruited into the tumor bed, in line with its previously reported capacity to promote the differentiation of hematopoietic stem cells (Barbosa et al., 2011) and the cardinal importance of purinergic receptors for DC differentiation in vitro (Wilkin et al., 2001). $CD11b^+Ly6C^{hi}Ly6G^-$ TILs were found to contain a subset of GMPs that became particularly enriched after chemotherapy, provided that CD39 was not expressed by cancer cells. In the absence of dying tumor cell-derived ATP, $CD11b^+Ly6C^{hi}Ly6G^-$ TILs (as well as their bone marrow-derived counterparts) preferentially differentiated into granulocytes. The capacity of anthracycline-treated cancer cells to skew the differentiation of $CD11b^+Ly6C^{hi}Ly6G^-$ TILs toward an inflammatory DC-like phenotype depended on ATP and purinergic receptors, both in vitro and in vivo. Altogether, these observations suggest a dual role for ATP in the tumor microenvironment. First, ATP would be essential for the recruitment of myeloid cells into the proximity of dying cells and, second, ATP would facilitate the local differentiation and maintenance of cells with the phenotype of inflammatory DCs.

Multiple distinct DC subsets have been involved in anticancer immunosurveillance (Palucka and Banchereau, 2012), and advanced tumors can actually convert tumor-infiltrating DCs into immunosuppressive cells (Gabrilovich et al., 2012). In the specific context of anthracycline-based chemotherapy, however, only inflammatory DC-like $CD11c^+CD11b^+Ly6C^{hi}$ cells were found to be essential for optimal immune system-mediated anticancer responses. Indeed, several distinct manipulations suppressing the accumulation of such inflammatory DC-like cells in the tumor bed also abolished the antitumor activity of anthracycline-based chemotherapy. In contrast, the depletion of pDCs, neutrophils, or macrophages with antibodies targeting PDCA-1 and Ly6G or clodronate-containing liposomes, as well as the elimination of Batf3-dependent DCs, had no major impact on chemotherapeutic responses. Intriguingly, inflammatory DCs, which are particularly important for chemotherapy-elicited immunosurveillance, can differentiate in response to HMGB1 (Han et al., 2008), suggesting that HMGB1 released from dying cancer cells may further contribute to the maturation and/or differentiation of TILs toward such phenotype. Irrespective of these possibilities, our results unravel the essential contribution of one particular DC-like subset, namely the $CD11c^+CD11b^+Ly6C^{hi}$ population, to the therapeutic anticancer immune response elicited by anthracyclines.

The question as to whether chemotherapy elicits de novo T cell priming and/or reactivates local effector and/or memory T cells remains elusive. As outlined by De Visser and colleagues (Ciampricotti et al., 2012), oncogene-addicted nonimmunogenic breast tumors fail to prime a significant T cell response when they are treated with anthracyclines. However, we speculate that chemotherapy-induced immunogenic cell death may at least reboot antigen-specific T cell responses that have been initiated prior to chemotherapy. Our findings indicate that (1) draining lymph nodes are dispensable for the immune system-mediated antitumor effects of anthracyclines, (2) inflammatory DCs accumulate within neoplastic lesions in response to anthracyclines, and these cells function as efficient APCs when extracted from tumor beds, and (3) no significant $CD8^+$ T cell (OT-I) priming against the immunodominant epitopes of OVA is detectable in the spleen and lungs by day 7 after chemotherapy (data not shown), although such response occurs within the tumor. In line with these notions, pegylated IL-10-based therapy has been shown to reactivate intratumoral cancer-specific cytotoxic $CD8^+$ TILs, to restore the in situ expression of Th1 cytokines, granzymes, and antigen-presentation molecules, and to culminate in the control of tumor growth, even in the absence of draining lymph nodes (Mumm et al., 2011). However, our data do not formally exclude the possibility that antigen presentation may take place at extratumoral sites, such as the bone marrow, to which tumor antigens may be transported by neutrophils (Duffy et al., 2012). Irrespective of this partially unresolved issue, we show here that anthracyclines promote a crucial ATP-dependent pathway whereby the intratumoral accumulation of GMPs and

(B and C) Quantitative data (means ± SEM); $^{**}p < 0.01$, $^{***}p < 0.001$ (unpaired, two-tailed Student's t test).
(D–F) Morphology of colonies generated from $CD11b^+Ly6C^{hi}$ TILs (scale bar represents 50 μm) (D), $Ki\text{-}67^+$ dots in the nucleus of cells, as assessed by immunofluorescence microscopy upon Hoechst 33342 counterstaining (scale bar represents 10 μm) (E), and May-Grünwald-Giemsa staining of a cytospin prepared from these cells (scale bar represents 5 μm, original magnification 400×) (F).
See also Figure S4.

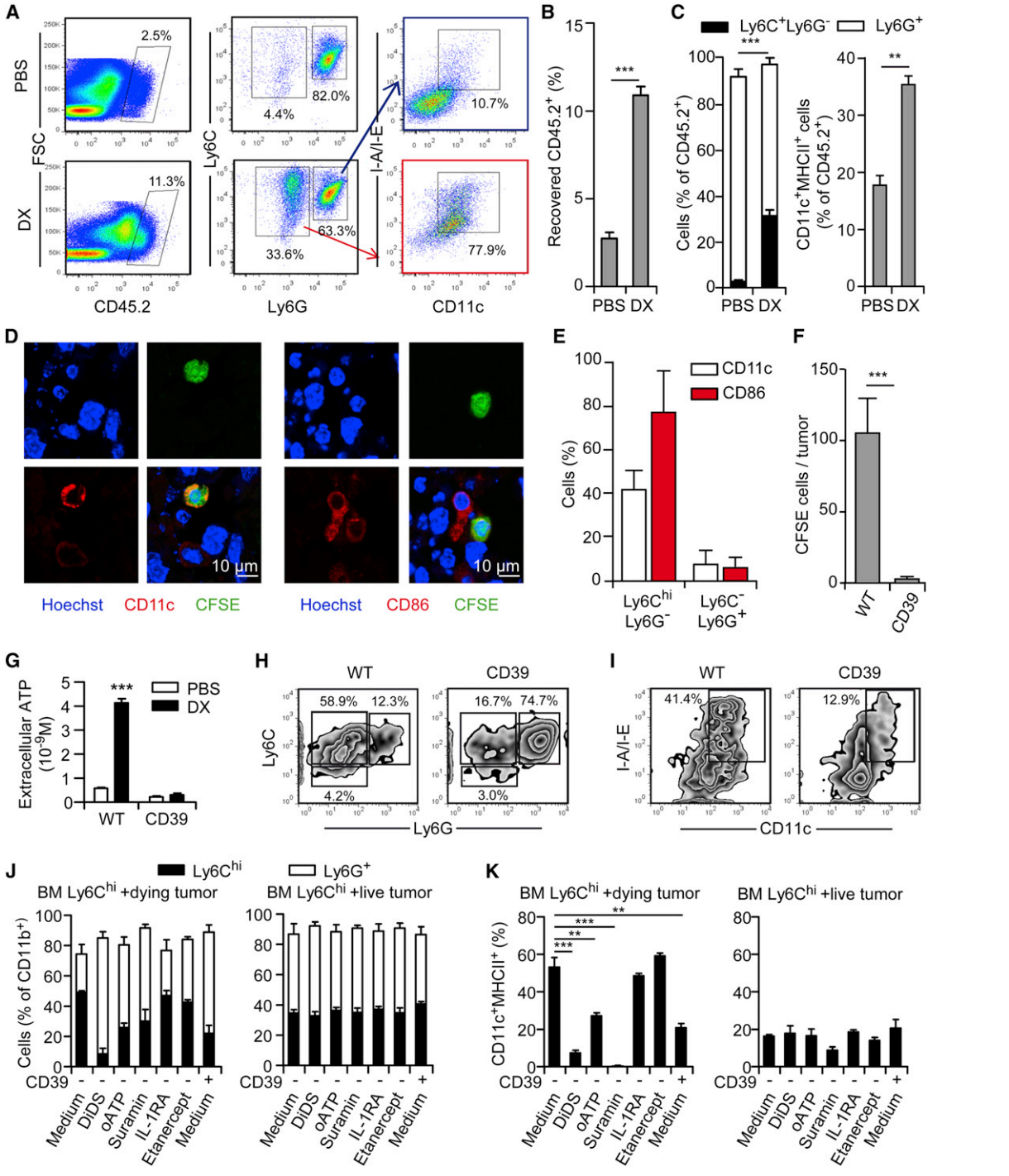

Figure 5. Chemotherapy-Induced and ATP-Dependent Differentiation of CD11b$^+$Ly6C^{hi} Tumor-Infiltrating Leucocytes into Inflammatory DC-like Cells

(A–C) CD11b$^+$Ly6C^{hi} cells purified from doxorubicin (DX)-treated tumors from C57BL/6 CD45.2 mice were injected into MCA205 tumors implanted in C57BL/6 CD45.1 mice that had been pretreated with DX i.t. or with an equivalent volume of PBS. After 48 hr, tumors were collected and the phenotype of transferred CD45.2$^+$ cells was analyzed by flow cytometry.

(A) Representative dot plots (numbers indicate the percentage of cells found within the corresponding gate).

(B and C) Quantitative data on the percentage of recovered CD45.2$^+$ cells (B) and on their differentiation into CD11b$^+$Ly6C$^+$Ly6G$^-$, CD11b$^+$Ly6G$^+$, or CD11c$^+$MHC-II$^+$ cells (C) (means ± SEM).

(D–F) CD11b$^+$Ly6C^{hi} or Ly6G$^+$ cells sorted from MCA205 fibrosarcomas treated with DX were labeled with CFSE and inoculated into wild-type (WT) or CD39-expressing (CD39) MCA205 fibrosarcomas that had been pretreated 48 hr earlier with mitoxantrone (MTX) i.p. or with an equivalent volume of PBS. 48 hr later, tumors from recipient mice were harvested and processed for immunofluorescence microscopy-assisted determinations. Representative images are depicted in

(legend continued on next page)

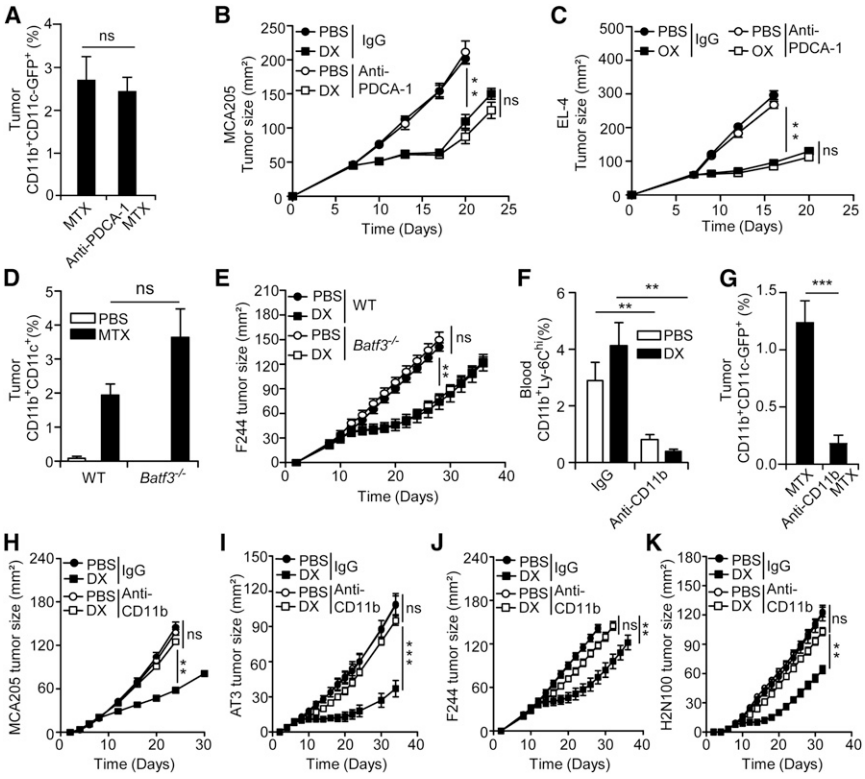

Figure 6. The Therapeutic Efficacy of Anthracyclines Relies on CD11b$^+$ Myeloid DCs but Neither on Plasmacytoid DCs nor on Batf3-Dependent DCs

(A) CD11c-DTR/GFP mice bearing wild-type (WT) MCA205 fibrosarcomas were treated with mitoxantrone (MTX) i.p., combined with either PDCA-1-specific or isotype control antibodies (IgGs). Nine days later, the percentage of CD11c$^+$CD11b$^-$GFP$^+$ tumor-infiltrating cells was determined by immunofluorescence microscopy. Quantitative data are reported as means ± SEM; ns, nonsignificant (unpaired, two-tailed Student's t test).

(B and C) C57BL/6 mice were inoculated with WT MCA205 fibrosarcoma (B) or EL-4 lymphoma (C) cells (day −7) and, on day 0, they were treated with doxorubicin (DX) i.t. (B) or oxaliplatin (OX) i.p. (C), combined with either PDCA-1-targeting antibodies or isotype control IgGs on days −1, 1, and 2. Tumor growth was routinely assessed throughout the experiment (n = 5–8 mice/group). Quantitative data are reported as means ± SEM; ns, nonsignificant, **p < 0.01 (Mann-Whitney U test).

(D) WT or *Batf3*$^{-/-}$ mice bearing F244 sarcomas were treated with MTX i.p. or an equivalent volume of PBS. Two days later, tumors were harvested and processed for the immunofluorescence microscopy-assisted detection of CD11b$^+$CD11c$^+$ DCs within the tumor bed (n = 4–5 mice/group). Quantitative data are reported as means ± SEM; ns, nonsignificant (unpaired, two-tailed Student's t test).

(E) WT or *Batf3*$^{-/-}$ 129/Sv mice were inoculated with WT F244 sarcoma cells (day −7) and, on day 0, they were treated with DX i.t. or an equivalent volume of PBS. Tumor growth was routinely assessed throughout the experiment (n = 5–8 mice/group). Quantitative data are reported as means ± SEM; ns, nonsignificant, **p < 0.01 (Mann-Whitney U test).

(F and G) CD11c-DTR/GFP mice bearing WT MCA205 fibrosarcomas were treated with MTX i.p., DX i.t., or with an equivalent volume of PBS, combined with either CD11b-specific antibodies or isotype control IgGs, which were administered 1 day before and on the same day as chemotherapy. 20 and 38 hr later, blood (F) and tumor (G) samples were collected and analyzed by flow cytometry and immunofluorescence microscopy, respectively, for the abundance of CD11b$^+$Ly6C^{hi} and CD11c$^+$CD11b$^-$GFP$^+$ cells, respectively. Quantitative data are reported as means ± SEM; **p < 0.01, ***p < 0.001 (unpaired, two-tailed Student's t test).

(H–K) C57BL/6 (H and I), 129/Sv (J), or BALB/c (K) mice were inoculated with WT MCA205 (H), AT3 (I), F244 (J), and H2N100 (K) cells (day = −7) and, on day 0, they were treated DX i.t. or an equivalent volume of PBS, combined with either CD11b-specific antibodies or isotype control IgGs (n > 5 mice/group). Quantitative data are reported as means ± SEM; ns, nonsignificant, **p < 0.01, ***p < 0.001 (Log-rank Mann-Whitney U test).

See also Figure S6.

inflammatory monocytes in fine facilitate the local differentiation of inflammatory DCs and the activation of T cells against cancer.

EXPERIMENTAL PROCEDURES

Tumor Chemotherapy Models

For the establishment of syngenic solid tumors, CB57BL/6 mice received EL-4, AT3, WT MCA205, or OVA-expressing MCA205 cells, BALB/c mice were inoculated with H2N100, WT CT26, or MyrPalm-mEGFP-expressing CT26 cells, and WT or *Batf3*$^{-/-}$ 129/Sv mice were engrafted with F244 cells. Tumor growth was then monitored routinely by means of a caliper, and when the tumor surface reached 25–45 mm^2 (day 0), mice received either DX, MTX, oxaliplatin, or equivalent volumes of solvent. When appropriate, mice received intravenous suramin or an equivalent volume of solvent, on the same day of chemotherapy. Alternatively, mice received on days −1, 0, and weekly thereafter until the end of the experiment CD11b-, PDCA-1-, or Ly6G-targeting antibodies. In some protocols, tumor-bearing mice received on day −1, 1, and twice weekly thereafter until the end of the experiment IL-7- or IL-7R-specific antibodies or LTβR-Fc fusion proteins (kindly provided by Y.-X. Fu, University of Chicago). All experiments were performed in accordance with the Federation of European Laboratory Animal Science Association (FELASA) guidelines and were approved either by the IGR Ethics Committee (CEEA IRCIV/IGR no. 26, registered with the French Ministry of Research) or by the Peter MacCallum Animal Experimentation Ethics Committee.

(D) (scale bars represent 10 μm), and quantitative data (means ± SEM, n = 2 independent experiments with 3–5 mice/group) are reported in (E) (percentage of CD11c$^+$ and CD86$^+$ cells) and (F) (number of CFSE$^+$ cells/tumor).

(G–K) WT and CD39 MCA205 tumor cells were treated with PBS or 25 μM DX for 20 hr, followed by the quantification of extracellular ATP by a luciferase-based assay (G) or the coculture with bone marrow-derived (BM) Ly6C^{hi}Ly6G$^-$ cells for 5 days in the presence of 5 ng/ml GM-CSF and 5 ng/ml IL-4, alone or combined with 10 μM 4,4′-diisothiocyano-2,2′-stilbenedisulfonic acid (DiDS), 500 μM oxidized ATP (oATP), 2 mM suramin, 20 μg/ml interleukin-1 receptor antagonist (IL-1RA), or 20 μg/ml etanercept (H–K). (H) and (I) depict dot plots representative of the commitment toward the monocytic (Ly6C$^+$Ly6G$^-$) or granulocytic (Ly6G$^+$) lineage, and toward a DC-like phenotype (CD11c$^+$MHCII$^+$), respectively. Numbers indicate the percentage of cells found within the corresponding gate. (J) and (K) summarize quantitative data (means ± SEM) on the percentage of monocytic (CD11b$^+$Ly6C^{hi}Ly6G$^-$) (J), granulocytic (CD11b$^+$Ly6G$^+$) (J), and DC-like (CD11c$^+$MHCII$^+$) (K) cells obtained.

**p < 0.01, ***p < 0.001 (unpaired, two-tailed Student's t test). See also Figure S5.

Lymphadenectomy

For lymph node removal, mice were anesthetized under continuous isoflurane flow and subjected to skin decontamination with 10% povidone-iodine (commercial Betadine solution). Thereafter, a narrow incision (3 mm) was made, and the inguinal lymph node was removed with dissecting forceps. Finally, the incision was closed with sterile skin closure clips. Sham-operated mice (without lymph node resection) were treated similarly, and the duration of surgery was standardized between the two groups. Placing mice on a heater plate set at 37°C until awakening facilitated recovery.

Colony-Forming Assays

Myeloid subpopulations sorted from tumors were resuspended in MethoCult GF M3434 medium (StemCell Technologies) and 1 ml cell suspension was dispensed into 35 mm vented Petri dishes (Greiner Bio-One) when bubbles dissipated. Cultures were then incubated for 7–14 days in standard conditions in the presence of sterile water to preserve humidity.

ATP Quantification

ATP in culture supernatants was quantified by means of the luciferin-based ENLITEN ATP Assay Kit (Promega), as per manufacturer's instructions, on a Fluostar multiwell plate reader (BMG Labtech).

Statistical Analyses

Unless otherwise indicated, results are expressed as means ± SEM of n = 3 parallel assessments. All experiments were repeated at least twice, yielding similar results. Normal distributions were compared by unpaired, two-tailed Student's t tests, and tumor growth curves were compared by the Mann-Whitney U test. Kaplan-Meier survival curves were analyzed with the log-rank test. Statistical analyses were performed by means of the software Prism 5 (GraphPad) or Excel 2007 (Microsoft). p values < 0.05 were considered as statistically significant.

SUPPLEMENTAL INFORMATION

Supplemental Information includes Supplemental Experimental Procedures and six figures and can be found with this article online at http://dx.doi.org/10.1016/j.immuni.2013.03.003.

ACKNOWLEDGMENTS

We thank P. Rameau and Y. Lécluse for assistance with flow cytometry, T. Tordjmann and J.-L. Villeval for discussion, and colleagues from the IGR animal facility. We acknowledge R. Schreiber for providing F244 tumor cells, A.D. Weinberg for OVA-expressing MCA205 cells, and K. Murphy for *Batf3*$^{-/-}$ mice. G.K. and L.Z. are supported by the European Commission (ArtForce), Agence National de la Recherche (ANR), Ligue contre le Cancer (Equipe labellisée), Fondation pour la Recherche Médicale (FRM), Institut National du Cancer (INCa), Association pour la Recherche sur le Cancer (ARC) LabEx Immuno-Oncologie, Fondation de France, Fondation Bettencourt-Schueller, AXA Chair for Longevity Research, Cancéropôle Ile-de-France, and Paris Alliance of Cancer Research Institutes (PACRI). Y.M. and H.Y. were supported by China Scholarship Council (CSC), S.A. and I.M. by Ligue Nationale contre le Cancer, J.P.P.C. by Coordenação de Aperfeicoamento Pessoal de Nível Superior (CAPES/Brazil), D.H. by ARC, and M.J.S. by a National Health and Medical Research Council (NH&MRC) Australia Fellowship and Program Grant and by a grant from the Victorian Cancer Agency. Y.M., S.A., S.R.M., T.Y., L.A., H.Y., J.P.P.C., D.H., H.D., K.S., I.M., F.S., M.M., O.K., A.Q.S., L.M., E.V., and N.D. performed experiments. Y.M., M.J.S., R.K., E.S., S.G., P.R.T., L.Z., and G.K. conceived the study. Y.M., S.A., L.G., L.Z., and G.K. wrote the paper.

Received: May 25, 2012
Accepted: December 6, 2012
Published: April 4, 2013

REFERENCES

Albert, M.L., Sauter, B., and Bhardwaj, N. (1998). Dendritic cells acquire antigen from apoptotic cells and induce class I-restricted CTLs. Nature *392*, 86–89.

Apetoh, L., Ghiringhelli, F., Tesniere, A., Obeid, M., Ortiz, C., Criollo, A., Mignot, G., Maiuri, M.C., Ullrich, E., Saulnier, P., et al. (2007). Toll-like receptor 4-dependent contribution of the immune system to anticancer chemotherapy and radiotherapy. Nat. Med. *13*, 1050–1059.

Auffray, C., Sieweke, M.H., and Geissmann, F. (2009). Blood monocytes: development, heterogeneity, and relationship with dendritic cells. Annu. Rev. Immunol. *27*, 669–692.

Barbosa, C.M., Leon, C.M., Nogueira-Pedro, A., Wasinsk, F., Araújo, R.C., Miranda, A., Ferreira, A.T., and Paredes-Gamero, E.J. (2011). Differentiation of hematopoietic stem cell and myeloid populations by ATP is modulated by cytokines. Cell Death Dis *2*, e165.

Borsellino, G., Kleinewietfeld, M., Di Mitri, D., Sternjak, A., Diamantini, A., Giometto, R., Höpner, S., Centonze, D., Bernardi, G., Dell'Acqua, M.L., et al. (2007). Expression of ectonucleotidase CD39 by Foxp3+ Treg cells: hydrolysis of extracellular ATP and immune suppression. Blood *110*, 1225–1232.

Casares, N., Pequignot, M.O., Tesniere, A., Ghiringhelli, F., Roux, S., Chaput, N., Schmitt, E., Hamai, A., Hervas-Stubbs, S., Obeid, M., et al. (2005). Caspase-dependent immunogenicity of doxorubicin-induced tumor cell death. J. Exp. Med. *202*, 1691–1701.

Chalmin, F., Mignot, G., Bruchard, M., Chevriaux, A., Végran, F., Hichami, A., Ladoire, S., Derangère, V., Vincent, J., Masson, D., et al. (2012). Stat3 and Gfi-1 transcription factors control Th17 cell immunosuppressive activity via the regulation of ectonucleotidase expression. Immunity *36*, 362–373.

Chekeni, F.B., Elliott, M.R., Sandilos, J.K., Walk, S.F., Kinchen, J.M., Lazarowski, E.R., Armstrong, A.J., Penuela, S., Laird, D.W., Salvesen, G.S., et al. (2010). Pannexin 1 channels mediate 'find-me' signal release and membrane permeability during apoptosis. Nature *467*, 863–867.

Chen, Y., Corriden, R., Inoue, Y., Yip, L., Hashiguchi, N., Zinkernagel, A., Nizet, V., Insel, P.A., and Junger, W.G. (2006). ATP release guides neutrophil chemotaxis via P2Y2 and A3 receptors. Science *314*, 1792–1795.

Cheong, C., Matos, I., Choi, J.H., Dandamudi, D.B., Shrestha, E., Longhi, M.P., Jeffrey, K.L., Anthony, R.M., Kluger, C., Nchinda, G., et al. (2010). Microbial stimulation fully differentiates monocytes to DC-SIGN/CD209(+) dendritic cells for immune T cell areas. Cell *143*, 416–429.

Chow, A., Brown, B.D., and Merad, M. (2011). Studying the mononuclear phagocyte system in the molecular age. Nat. Rev. Immunol. *11*, 788–798.

Ciampricotti, M., Hau, C.S., Doornebal, C.W., Jonkers, J., and de Visser, K.E. (2012). Chemotherapy response of spontaneous mammary tumors is independent of the adaptive immune system. Nat. Med. *18*, 344–346, author reply 346.

de la Luz Sierra, M., Sakakibara, S., Gasperini, P., Salvucci, O., Jiang, K., McCormick, P.J., Segarra, M., Stone, J., Maric, D., Zhu, J., et al. (2010). The transcription factor Gfi1 regulates G-CSF signaling and neutrophil development through the Ras activator RasGRP1. Blood *115*, 3970–3979.

Denkert, C., Loibl, S., Noske, A., Roller, M., Müller, B.M., Komor, M., Budczies, J., Darb-Esfahani, S., Kronenwett, R., Hanusch, C., et al. (2010). Tumor-associated lymphocytes as an independent predictor of response to neoadjuvant chemotherapy in breast cancer. J. Clin. Oncol. *28*, 105–113.

Duffy, D., Perrin, H., Abadie, V., Benhabiles, N., Boissonnas, A., Liard, C., Descours, B., Reboulleau, D., Bonduelle, O., Verrier, B., et al. (2012). Neutrophils transport antigen from the dermis to the bone marrow, initiating a source of memory CD8+ T cells. Immunity *37*, 917–929.

Elliott, M.R., Chekeni, F.B., Trampont, P.C., Lazarowski, E.R., Kadl, A., Walk, S.F., Park, D., Woodson, R.I., Ostankovich, M., Sharma, P., et al. (2009). Nucleotides released by apoptotic cells act as a find-me signal to promote phagocytic clearance. Nature *461*, 282–286.

Gabrilovich, D.I., Ostrand-Rosenberg, S., and Bronte, V. (2012). Coordinated regulation of myeloid cells by tumours. Nat. Rev. Immunol. *12*, 253–268.

Galluzzi, L., Vitale, I., Abrams, J.M., Alnemri, E.S., Baehrecke, E.H., Blagosklonny, M.V., Dawson, T.M., Dawson, V.L., El-Deiry, W.S., Fulda, S., et al. (2012). Molecular definitions of cell death subroutines: recommendations of the Nomenclature Committee on Cell Death 2012. Cell Death Differ. *19*, 107–120.

Gardai, S.J., McPhillips, K.A., Frasch, S.C., Janssen, W.J., Starefeldt, A., Murphy-Ullrich, J.E., Bratton, D.L., Oldenborg, P.A., Michalak, M., and

Henson, P.M. (2005). Cell-surface calreticulin initiates clearance of viable or apoptotic cells through trans-activation of LRP on the phagocyte. Cell *123*, 321–334.

Ghiringhelli, F., Apetoh, L., Tesniere, A., Aymeric, L., Ma, Y., Ortiz, C., Vermaelen, K., Panaretakis, T., Mignot, G., Ullrich, E., et al. (2009). Activation of the NLRP3 inflammasome in dendritic cells induces IL-1beta-dependent adaptive immunity against tumors. Nat. Med. *15*, 1170–1178.

Gräbner, R., Lötzer, K., Döpping, S., Hildner, M., Radke, D., Beer, M., Spanbroek, R., Lippert, B., Reardon, C.A., Getz, G.S., et al. (2009). Lymphotoxin beta receptor signaling promotes tertiary lymphoid organogenesis in the aorta adventitia of aged ApoE-/- mice. J. Exp. Med. *206*, 233–248.

Green, D.R., Ferguson, T., Zitvogel, L., and Kroemer, G. (2009). Immunogenic and tolerogenic cell death. Nat. Rev. Immunol. *9*, 353–363.

Han, J., Zhong, J., Wei, W., Wang, Y., Huang, Y., Yang, P., Purohit, S., Dong, Z., Wang, M.H., She, J.X., et al. (2008). Extracellular high-mobility group box 1 acts as an innate immune mediator to enhance autoimmune progression and diabetes onset in NOD mice. Diabetes *57*, 2118–2127.

Hildner, K., Edelson, B.T., Purtha, W.E., Diamond, M., Matsushita, H., Kohyama, M., Calderon, B., Schraml, B.U., Unanue, E.R., Diamond, M.S., et al. (2008). Batf3 deficiency reveals a critical role for CD8alpha+ dendritic cells in cytotoxic T cell immunity. Science *322*, 1097–1100.

Kool, M., Soullié, T., van Nimwegen, M., Willart, M.A., Muskens, F., Jung, S., Hoogsteden, H.C., Hammad, H., and Lambrecht, B.N. (2008). Alum adjuvant boosts adaptive immunity by inducing uric acid and activating inflammatory dendritic cells. J. Exp. Med. *205*, 869–882.

Kroemer, G., Galluzzi, L., and Brenner, C. (2007). Mitochondrial membrane permeabilization in cell death. Physiol. Rev. *87*, 99–163.

Ladoire, S., Mignot, G., Dabakuyo, S., Arnould, L., Apetoh, L., Rébé, C., Coudert, B., Martin, F., Bizollon, M.H., Vanoli, A., et al. (2011). In situ immune response after neoadjuvant chemotherapy for breast cancer predicts survival. J. Pathol. *224*, 389–400.

Laslo, P., Spooner, C.J., Warmflash, A., Lancki, D.W., Lee, H.J., Sciammas, R., Gantner, B.N., Dinner, A.R., and Singh, H. (2006). Multilineage transcriptional priming and determination of alternate hematopoietic cell fates. Cell *126*, 755–766.

Ma, Y., Aymeric, L., Locher, C., Mattarollo, S.R., Delahaye, N.F., Pereira, P., Boucontet, L., Apetoh, L., Ghiringhelli, F., Casares, N., et al. (2011). Contribution of IL-17-producing gamma delta T cells to the efficacy of anticancer chemotherapy. J. Exp. Med. *208*, 491–503.

Martins, I., Tesniere, A., Kepp, O., Michaud, M., Schlemmer, F., Senovilla, L., Séror, C., Métivier, D., Perfettini, J.L., Zitvogel, L., and Kroemer, G. (2009). Chemotherapy induces ATP release from tumor cells. Cell Cycle *8*, 3723–3728.

Matta, B.M., Castellaneta, A., and Thomson, A.W. (2010). Tolerogenic plasmacytoid DC. Eur. J. Immunol. *40*, 2667–2676.

Meier, D., Bornmann, C., Chappaz, S., Schmutz, S., Otten, L.A., Ceredig, R., Acha-Orbea, H., and Finke, D. (2007). Ectopic lymphoid-organ development occurs through interleukin 7-mediated enhanced survival of lymphoid-tissue-inducer cells. Immunity *26*, 643–654.

Mellman, I., Coukos, G., and Dranoff, G. (2011). Cancer immunotherapy comes of age. Nature *480*, 480–489.

Michaud, M., Martins, I., Sukkurwala, A.Q., Adjemian, S., Ma, Y., Pellegatti, P., Shen, S., Kepp, O., Scoazec, M., Mignot, G., et al. (2011). Autophagy-dependent anticancer immune responses induced by chemotherapeutic agents in mice. Science *334*, 1573–1577.

Mumm, J.B., Emmerich, J., Zhang, X., Chan, I., Wu, L., Mauze, S., Blaisdell, S., Basham, B., Dai, J., Grein, J., et al. (2011). IL-10 elicits IFNγ-dependent tumor immune surveillance. Cancer Cell *20*, 781–796.

Obeid, M., Tesniere, A., Ghiringhelli, F., Fimia, G.M., Apetoh, L., Perfettini, J.L., Castedo, M., Mignot, G., Panaretakis, T., Casares, N., et al. (2007). Calreticulin exposure dictates the immunogenicity of cancer cell death. Nat. Med. *13*, 54–61.

Palucka, K., and Banchereau, J. (2012). Cancer immunotherapy via dendritic cells. Nat. Rev. Cancer *12*, 265–277.

Panaretakis, T., Kepp, O., Brockmeier, U., Tesniere, A., Bjorklund, A.C., Chapman, D.C., Durchschlag, M., Joza, N., Pierron, G., van Endert, P., et al. (2009). Mechanisms of pre-apoptotic calreticulin exposure in immunogenic cell death. EMBO J. *28*, 578–590.

Pérarnau, B., Saron, M.F., Reina San Martin, B., Bervas, N., Ong, H., Soloski, M.J., Smith, A.G., Ure, J.M., Gairin, J.E., and Lemonnier, F.A. (1999). Single H2Kb, H2Db and double H2KbDb knockout mice: peripheral CD8+ T cell repertoire and anti-lymphocytic choriomeningitis virus cytolytic responses. Eur. J. Immunol. *29*, 1243–1252.

Schreiber, R.D., Old, L.J., and Smyth, M.J. (2011). Cancer immunoediting: integrating immunity's roles in cancer suppression and promotion. Science *331*, 1565–1570.

Stagg, J., and Smyth, M.J. (2010). Extracellular adenosine triphosphate and adenosine in cancer. Oncogene *29*, 5346–5358.

Wilkin, F., Duhant, X., Bruyns, C., Suarez-Huerta, N., Boeynaems, J.M., and Robaye, B. (2001). The P2Y11 receptor mediates the ATP-induced maturation of human monocyte-derived dendritic cells. J. Immunol. *166*, 7172–7177.

Yegutkin, G.G., Samburski, S.S., and Jalkanen, S. (2003). Soluble purine-converting enzymes circulate in human blood and regulate extracellular ATP level via counteracting pyrophosphatase and phosphotransfer reactions. FASEB J. *17*, 1328–1330.

Yu, M., Riva, L., Xie, H., Schindler, Y., Moran, T.B., Cheng, Y., Yu, D., Hardison, R., Weiss, M.J., Orkin, S.H., et al. (2009). Insights into GATA-1-mediated gene activation versus repression via genome-wide chromatin occupancy analysis. Mol. Cell *36*, 682–695.

Zappasodi, R., Pupa, S.M., Ghedini, G.C., Bongarzone, I., Magni, M., Cabras, A.D., Colombo, M.P., Carlo-Stella, C., Gianni, A.M., and Di Nicola, M. (2010). Improved clinical outcome in indolent B-cell lymphoma patients vaccinated with autologous tumor cells experiencing immunogenic death. Cancer Res. *70*, 9062–9072.